Available online at www.sciencedirect.com
SCIENCE DIRECT®
International Journal of Multiphase Flow 32 (2006) 248–268
International Journal of Multiphase Flow
www.elsevier.com/locate/ijmulflow

Averaging of particle data from phase Doppler anemometry in unsteady two-phase flow: Validation by numerical simulation

Tobias Bergenblock [a,*], Bo Leckner [a], Fabrice Onofri [b], René Occelli [b], Lounès Tadrist [b]

[a] *Chalmers University of Technology, Department of Energy Conversion, SE-412 96 Göteborg, Sweden*
[b] *IUSTI-CNRS, University of Provence, Technopole de Chateau Gombert, 5, rue Enrico Fermi, 13453 Marseille Cedex 13, France*

Received 29 March 2005; received in revised form 17 October 2005

Abstract

A novel post-processing algorithm is proposed to correct statistical bias observed in the treatment of time series obtained by a phase Doppler anemometer (PDA) at flow locations with variable particle velocity and concentration. Extensive properties of each validated particle are weighted with their inverse measuring (validation) volume to account for the procedure of particle sampling and fluctuations in the particle concentration. To compensate for the short characteristic length of the validation volume, the properties of particles are expressed by properties of fields of particle groups, using a local averaging time. A window shift and a decorrelation scheme are applied on the fields to increase their frequency resolution. This algorithm has been tested on numerical time series, provided by an Eulerian/Lagrangian code representing a gas/solids flow past a bluff body. Moments and spectral estimates of concentration and velocity of particle groups were successfully validated by the numerical simulation using the PDA data algorithm and control volume averaging. The control volume was much larger than the PDA validation volume, but the centre positions of the two volumes were identical.

Keywords: Phase Doppler anemometry; Two-phase flow; Particle groups; Eulerian/Lagrangian simulation; Bluff body

1. Introduction

It is of interest to characterize disperse two-phase flows in terms of moments of velocity and concentration of particles. Phase Doppler anemometry (PDA) provides the possibility of such a characterization in dilute flows of embedded spherical particles. The concentration of the disperse phase may vary in time and space and mean quantities have to be defined. The straightforward definition of a mean quantity is the

* Corresponding author. Tel.: +46 31 772 1437; fax: +46 31 772 3592.
E-mail address: tober@chalmers.se (T. Bergenblock).

0301-9322/$ - see front matter © 2005 Elsevier Ltd. All rights reserved.
doi:10.1016/j.ijmultiphaseflow.2005.10.003

mass-weighted average (Pope, 1985). However, laser Doppler anemometry (LDA), which uses burst type of signal processing, suffers from velocity-dependent sampling rate (McLaughlin and Tiederman, 1973; Buchhave, 1975; George, 1975); the probability of sampling a particle depends on the velocity of the particle. In a flow-point, there is a higher probability to sample particles having high velocity than those of low velocity, even if there are equal numbers of slow and fast particles in the flow domain (uniformly or purely randomly distributed in space). Furthermore, the sampling rate may be correlated with the direction of the particle's movement (George, 1975), and this should also be accounted for. The velocity-dependent sampling rate is not corrected automatically, since the information about the sampled particle is only saved as one event that represents the entire passage through the detection volume. A hot wire applied to a turbulent single-phase flow also experiences more fast fluid elements than slow ones. The fast elements do not, however, remain in the neighbourhood of the wire as long as the slow ones, and for this reason unbiased time-averages can be estimated (George, 1975). For accurate estimation of the statistics of particle properties in a measurement point, optically accessible by an LDA, the maximum allowable particle loading is limited by the number of particles in the probe volume and the number entering the probe region during the transit time of a particle. These average numbers should be smaller than the order 10^{-2} (Edwards and Marx, 1992).

There are several well-known moment estimators for single-phase flows, related to ensemble, arrival time, and particle transit time (McLaughlin and Tiederman, 1973; Buchhave et al., 1979), to correct for the velocity-dependent sampling procedure of the LDA technique. The most general and successful method is weighting of the residence times of tracer particles in the measurement volume (Buchhave et al., 1979), provided that the residence time can be accurately measured. These methods of correction for bias have been investigated and validated using data simulation, mainly autoregressive models (Tropea, 1987; Fuchs et al., 1994), to generate flow fields. In disperse two-phase flows, additional complexities arise and should be taken into account: (i) on a micro scale, (a) the mass or volume of a particle may be correlated with local velocity (through gravity and/or drag), (b) several particles may occur in the sampling volume during the passage of a particle, since particles may prefer to move in groups and not purely randomly, (ii) on a meso-scale, the local density of coherent structures (clusters) may be correlated with the velocity of the structures. The effects of such complexities can be small, but not negligible, and they may affect the performance of statistical estimators of PDA data. This is not easily investigated using autoregressive models. Instead, a method is introduced here, in which a computer code describing the movement of discrete particles and interactions between particles and fluid, as well as between particles and particles like collisions (four-way coupling), is utilized to simulate a test case, where a simple PDA detection volume is placed in the flow. All micro and meso-scale correlations mentioned above are considered.

In several works dealing with measurements in unsteady two-phase flows, such as fluidized beds (Levy and Lockwood, 1983; Hamdullahpur and Mackay, 1986; Berkelmann and Renz, 1991; Yang et al., 1992; Wang et al., 1993; Zhang and Arastoopour, 1995; Samuelsberg and Hjertager, 1996; Werther et al., 1996; Van den Moortel et al., 1997, 1998; Mathiesen et al., 2000; Ibsen et al., 2001, 2004), the particle sampling procedure of the LDA and the fluctuating particle concentration were not considered. In such cases, measurement results in terms of moments of particle velocities can be expected to be biased towards high values. Two methods (Hardalupas and Horender, 2001; Bergenblock and Leckner, 2004) can be applied to PDA data obtained in fluctuating, low-speed applications, where some velocities of particles are allowed to be near zero, to estimate meso-scale flow fluctuations. Hardalupas and Horender (2001) introduced an algorithm for estimating first and second moments of droplet density (number, data rate, and volume) for quantification of deterministic stray unsteadiness. In their algorithm, as well as in previous ones based on local averaging time (van de Wall and Soo, 1994, 1997; Bao and Soo, 1996), the choice of the averaging time was rather arbitrary (the inverse averaging time should be smaller than the mean sampling rate and greater than the frequency of the flow fluctuations to be captured), and the variance of the estimated properties of a particle group depends on the choice of the local averaging time (van de Wall and Soo, 1994; Hardalupas and Horender, 2001). In the other algorithm (Bergenblock and Leckner, 2004), the local averaging time was chosen to be smaller than the integral time scale of particle velocity fluctuations (not to introduce additional correlation into meso-scale averages). The purpose was to estimate moments and spectral properties of the disperse phase in such two-phase flows, where properties of adjacent particles are correlated. The method was introduced in one dimension (in one velocity direction) on a particle-group scale and applied to a time series, detected by a phase

Doppler particle analyzer (PDA) in the dilute zone of a fluidized bed (Bergenblock et al., 2004). The processed mean particle velocity in the vertical direction was found to be as low as about 1/3 of the ensemble average particle velocity.

Here, the merits of these two algorithms (Hardalupas and Horender, 2001; Bergenblock and Leckner, 2004) are used to develop a reliable method for the estimation of instantaneous properties of particle groups, as well as up to second order moments of time-varying velocity and concentration of particle flow. The algorithm is validated by a two-dimensional numerical simulation, yielding simultaneous time series (of about 100 s) in a PDA detection volume and in a much larger control volume (CV) of a gas flow containing mono-disperse particles passing a bluff body. The PDA volume was located inside the CV volume. The flow was considered pseudo-3D using the particle diameter as the third dimension when estimating the drag force between gas and particle and the solids volume concentration. Adoption of this pseudo-3D assumption instead of a true third dimension has no major influence on the results of the validation of the algorithm, but it reduces the number of particles to be sampled and, hence, the simulation time needed to achieve an accurate description of the PDA validation volume. The mono-disperse simulation does not allow investigation of the correlation between particle size and PDA volume or velocity. Instead the dependence of concentration on the velocity of particle groups is emphasized.

The numerical simulation provides well-defined detection/CV volumes without experimental noise. Thus, the time-moments and spectral behaviour of particle properties, using spatial averaging over CV, are known and can be used to validate the algorithm proposed for the estimation of moments and spectral properties of PDA data.

In Section 2 the PDA data post-processing algorithm is presented. The validation of this post-processing algorithm, using the discrete particle simulation, is described in Section 3. Section 4 presents a test case, whereas the results and discussion of the CV and PDA simulations can be found in Section 5.

2. Theory

The post-processing algorithm employed to estimate long-time moments of intensive properties of PDA data is first introduced on a micro (particle) scale in Section 2.1. Then Section 2.2 presents the equations on a meso (particle group) scale, which allows the estimation of instantaneous values of such data in statistically stationary two-phase flow with a velocity that varies with time.

2.1. Micro scale

The mass-weighted ensemble average velocity of the entire PDA time series can be expressed as

$$\langle u \rangle^{\mathrm{m}} = \sum_{i=1}^{N} m_i u_i \Big/ \sum_{i=1}^{N} m_i \tag{1}$$

where m_i and u_i are the mass and velocity (in one direction) of particle i. This average does not account for the velocity-dependent sampling rate and fluctuating particle concentration and may contain high-velocity bias in high-intensity turbulent two-phase flows. In addition, the spatial extent of the PDA validation volume encountered by a particle depends both on direction of trajectory and on particle size. The exact spatial position of a particle in the detection volume is unknown by the receiving optics and software of the PDA. The length l of the particle trajectory through the validation volume is estimated from the absolute value of the velocity vector, $\mathbf{u}_i = (u_i, v_i, w_i)$, times the residence time, Δt_i, of the particle i in the volume. This estimation requires a constant particle velocity along the trajectory and an accurate determination of the velocity vector and the residence time of the particle. This is difficult to accomplish in complex optically dense 3D flows, and therefore, in the following a statistical procedure is proposed.

The validation volume of the PDA can be estimated (Sommerfeld and Qiu, 1995) from the maximum amplitude of the Doppler burst and its integral energy above a given threshold, but this method cannot be applied to commercial systems. Here, instead, the validation volume $V_{(d,\gamma)\text{-}i}$ encountered by particle i is estimated by an automatic calibration procedure (Saffman, 1987; Roisman and Tropea, 2001). $V_{(d,\gamma)\text{-}i}$ is approximated from

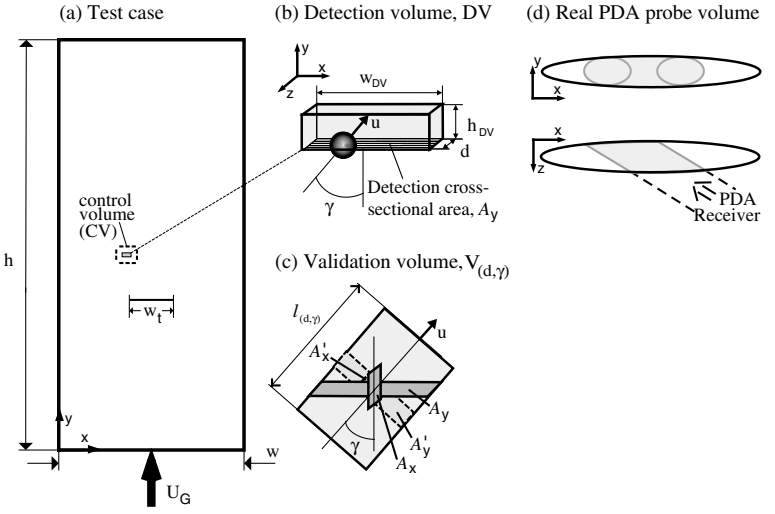

Fig. 1. (a) Schematic drawing (not to scale) of the test case, showing the riser with a confined bluff body of width w_t, and a close-up of a detected particle, inside the control volume, in the (b) detection volume (rectangloid), as well as (c) corresponding validation volume and (d) a real PDA probe volume. Shaded areas correspond to volumes of possible particle detection.

the average path length, $l_{(d,\gamma)}$, of a valid particle in the detection volume, associated with the diameter of the particle and the path angle (d,γ) (γ is the angle between the velocity vector of the particle and the main flow direction), multiplied by the cross-sectional area, $A_{(d,\gamma)\text{-}i}$, projected perpendicular to the velocity vector of the sampled particle, $\mathbf{u}_i$, see Fig. 1c,

$$V_{(d,\gamma)\text{-}i} = A_{(d,\gamma)\text{-}i} l_{(d,\gamma)\text{-interp.}} \tag{2}$$

The length, $l_{(d,\gamma)\text{-interp.}}$ of $V_{(d,\gamma)\text{-}i}$ in Eq. (2) can be estimated by a suitable scheme for interpolation between adjacent classes of particle size and trajectory angle, $l_{(d,\gamma)\text{-}j}$, where there should be enough particles (n_j) in each class (j) for an ensemble average to be representative,

$$l_{(d,\gamma)\text{-}j} = \frac{1}{n_j} \sum_{i=1}^{n_j} \Delta t_{(d,\gamma)\text{-}i} |\mathbf{u}_{(d,\gamma)\text{-}i}| \tag{3}$$

In Eq. (3), the ensemble average is calculated from all absolute values of the velocity vector of the detected and valid particles times the residence times of particles belonging to the same size and trajectory angle class (j). Neglecting the impact of the instantaneous particle concentration on the optical thickness of the suspension, the cross-sectional area, $A_{(d,\gamma)\text{-}i}$ of Eq. (2), is taken to vary with particle size, direction of particle path, optical setup, and measuring conditions. It is estimated using an approach by Roisman and Tropea (2001).

The validation volume is not constant for a PDA time series. This has serious consequences on the type of averaging that can be performed. The average concentration over a time T, (sufficiently long to form a statistically steady state) of an intensive property q, with its extensive mass-based equivalence P, is

$$\overline{q_{\text{p-micro}}} = \overline{\left(\frac{P}{\rho_\text{p} V}\right)} = \frac{1}{T}\int_0^T \left(\frac{1}{\rho_\text{p} V_{(d,\gamma)}} \int_{V_{(d,\gamma)}} P \,\mathrm{d}V\right) \mathrm{d}t \approx \frac{1}{T}\int_0^T \left(\sum_{i=1}^{N} \frac{P_i}{\rho_\text{p} V_{(d,\gamma)\text{-}i}}\right) \mathrm{d}t \approx \frac{1}{T}\sum_{i=1}^{N} \frac{P_i \Delta t_i}{\rho_\text{p} V_{(d,\gamma)\text{-}i}} \tag{4a}$$

where Δt_i is the transit time in the validation volume associated with particle i. N is the number of samples in the time series. Each extensive property, P_i, is made intensive by an extensive average (i.e. an average over the validation volume) to account for the particle velocity and size-dependent validation volume. The material density of the particles, ρ_p, is taken as constant throughout this work, as usually required by the PDA optics. The time-average property q is independent of the PDA sampling process if the probability of the presence of multiple particles is small in the detection volume during Δt_i, and if the difficulties associated with particles passing the boundaries of the detection volume are negligible. With an accurate time-average property q of Eq. (4a), measurements of local particle concentration, $q = c_\text{v}$, can be compared with numerical simulations if c_v is defined on similar length scales in the two cases. For high-speed flows, Eq. (4a) can be simplified to

$$\overline{q_{\text{p-micro}}} \approx \frac{1}{T}\sum_{i=1}^{N}\frac{P_i\Delta t_i}{\rho_{\text{p}}V_{(d,\gamma)\text{-}i}} \approx \frac{1}{T}\sum_{i=1}^{N}\frac{P_i}{\rho_{\text{p}}A_{(d,\gamma)\text{-}i}|\mathbf{u}|_i} \tag{4b}$$

in which the residence time Δt_i (sensitive to noise) is cancelled out since the length $l_{(d,\gamma)\text{-interp.}}$ of $V_{(d,\gamma)\text{-}i}$ (see Eq. (2)) is replaced with the instantaneous value $\Delta t_i|\mathbf{u}|_i$. Eq. (4b) can not deal with particle velocities near zero, which may be present in fluctuating low-speed flows (such as the flow investigated below), but the equation can be used to derive a particle-group approach capable of estimating the time-average property q in such low-speed flows.

In contrast to the ensemble average velocity of Eq. (1), an unbiased first velocity moment of PDA data can be derived by means of Eq. (4a) considering the varying particle concentration and velocity-dependent sampling rate. Hence, the time-averaged mass-weighted velocity of particle flow $U^{\text{m}}_{\text{micro}}$ is calculated as $U^{c_{\text{v}}}_{\text{micro}}$, weighted with solids volume concentration,

$$\overline{U^{\text{m}}_{\text{micro}}} \approx \overline{U^{c_{\text{v}}}_{\text{micro}}} = \left(\overline{q_{\text{p-micro}}}\right)_{q_{\text{p}}=c_{\text{v}}u} \Big/ \left(\overline{q_{\text{p-micro}}}\right)_{q_{\text{p}}=c_{\text{v}}} \approx \frac{1}{T}\sum_{i=1}^{N}\frac{m_iu_i\Delta t_i}{\rho_{\text{p}}V_{(d,\gamma)\text{-}i}} \Big/ \frac{1}{T}\sum_{i=1}^{N}\frac{m_i\Delta t_i}{\rho_{\text{p}}V_{(d,\gamma)\text{-}i}} \tag{5}$$

where u_i is a velocity component associated with particle i. The local extensive particle properties (mass, momentum, etc.) must be weighted with their associated validation volume $V_{(d,\gamma)\text{-}i}$, and hence the mass-weighted extensive properties are weighted by c_{v}. This is valid under the assumption of local spatial homogeneity, i.e. the local c_{v} value should be independent of the size of its instantaneous validation volume. However, only one particle is allowed in the validation volume during the particle's transit, and a change in size of the PDA detection volume on a micro scale affects the instantaneous value of c_{v}. Thus, an increase in the detection volume is likely to yield more non-valid particles, because the probability of presence of multiple particles increases.

It is tempting to write the equations for the root time-mean square (RMS) values of q_{p} and velocity on a micro level similar to the time-means,

$$\overline{q_{\text{p-micro}}}' = \left\{\frac{1}{T}\int_0^T\left[\sum_{i=1}^{N}\left(\frac{P_i}{\rho_{\text{p}}V_{(d,\gamma)\text{-}i}} - \overline{q_{\text{p-micro}}}\right)^2\right]\mathrm{d}t\right\}^{1/2} \approx \left\{\frac{1}{T}\left[\sum_{i=1}^{N}\left(\frac{P_i}{\rho_{\text{p}}V_{(d,\gamma)\text{-}i}} - \overline{q_{\text{p-micro}}}\right)^2\Delta t_i\right]\right\}^{1/2} \tag{6}$$

$$\overline{U^{\text{m}}_{\text{micro}}}' \approx \overline{U^{c_{\text{v}}}_{\text{micro}}}' = \frac{\left(\overline{q_{\text{p-micro}}}'\right)_{q_{\text{p}}=c_{\text{v}}u}}{\left(\overline{q_{\text{p-micro}}}'\right)_{q_{\text{p}}=c_{\text{v}}}} \approx \frac{\left\{\frac{1}{T}\left[\sum_{i=1}^{N}\left(\frac{m_iu_i}{\rho_{\text{p}}V_{(d,\gamma)\text{-}i}} - \overline{(c_{\text{v}}u)_{\text{micro}}}\right)^2\Delta t_i\right]\right\}^{1/2}}{\left\{\frac{1}{T}\left[\sum_{i=1}^{N}\left(\frac{m_i}{\rho_{\text{p}}V_{(d,\gamma)\text{-}i}} - \overline{(c_{\text{v}})_{\text{micro}}}\right)^2\Delta t_i\right]\right\}^{1/2}} \tag{7}$$

However, Eqs. (4)–(7) are not defined on large enough a volume to correctly estimate fluctuations in $q_{\text{p-micro}}$ and therefore Eqs. (6) and (7) will overpredict the time-RMS values. If the PDA data are accurate, the first moments (Eqs. (4a) and (5)) derived on a micro scale are expected to be good representations of the true time-averages, whereas the second moments (Eqs. (6) and (7)) are calculated on too small a volume, yielding a possible overprediction. Thus, if fluctuations in the flow are to be captured, and also if spectral analysis is to be performed (in which equi-spaced samples are preferred), it may be necessary to describe the flow on a larger scale, on a meso-scale (index meso). In addition, if particle groups are to be described, the extensive average of Eq. (4a) over $V_{(d,\gamma)}$ is performed on too short a length scale (a micro scale of similar length as the particle diameter) to be physically representative. Therefore, the average should be performed on a much larger scale than the characteristic dimension of the phase, a meso-scale.

2.2. Meso-scale

The time-average of an intensive property q_{p} on a meso-scale is defined by a constant local averaging time, Δt_{meso} (see Figs. 2 and 3) applied on Eq. (4a),

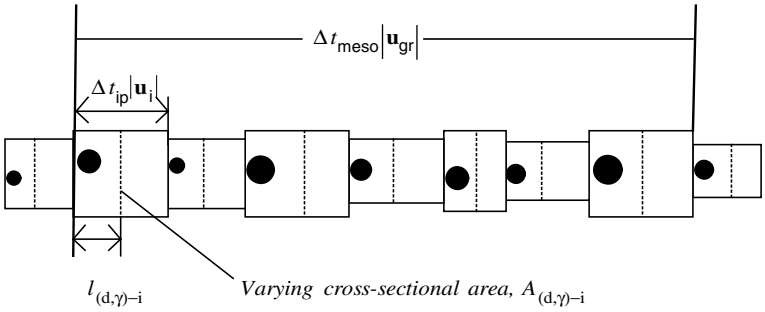

Fig. 2. Sketch of a particle group (black circles) encountered by a PDA system. The length $l_{(d,\gamma)\text{-}i}$ and cross-sectional area $A_{(d,\gamma)\text{-}i}$ of every validation volume are indicated, as well as the inter-particle $\Delta t_{ip}|\mathbf{u}_i|$ and group $\Delta t_{meso}|\mathbf{u}_{gr}|$ lengths.

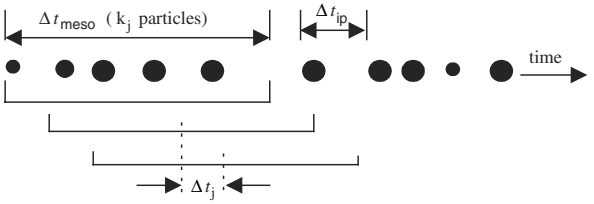

Fig. 3. Time average over a window of Δt_{meso} forming a particle group with a window shift Δt_j.

$$\overline{q_{p\text{-}meso}} \approx \frac{1}{T}\sum_{i=1}^{K_n}\frac{P_i\Delta t_i}{\rho_p V_{(d,\gamma)\text{-}i}} \approx \frac{1}{n}\sum_{j=1}^{n}\left(\frac{1}{\Delta t_{meso}}\sum_{i=K_{j-1}+1}^{K_j}\frac{P_i\Delta t_i}{\rho_p V_{(d,\gamma)\text{-}i}}\right)_j = \frac{1}{n}\sum_{j=1}^{n}\overline{q_{p\text{-}meso\text{-}j}} \tag{8}$$

where the local time-average (j) is performed over $k_j = K_j - K_{j-1}$ ($K_0 = 0$) particles (with correlated values of the property) to increase the length scale and to achieve an instantaneous estimate of q_p. n is number of meso-scale averages and K_n is total amount of particles in the time series (denoted N for micro scale properties in Section 2.1). The Δt_{meso} is chosen to be less than, or equal to, the smallest average integral time scale of fluctuations in the flow variables (e.g. particle concentration). In this way correlation added into the locally averaged data will not be excessive, see Section 5.3.2. The meso-averaging time acts as a filter, separating low and high-frequency fluctuations at the frequency $1/\Delta t_{meso}$. In Eq. (8), the time-average $\overline{q_{p\text{-}meso\text{-}j}}$ of the intensive property results in an ensemble average on a meso-level, $\overline{q_{p\text{-}meso}}$.

Alternatively, the time-average of an intensive property q_p can be estimated using Eq. (4b) and applying ensemble summation on the extensive property P_i of $k_j = K_j - K_{j-1}$ particles within Δt_{meso},

$$\overline{q_{p\text{-}gr}} \approx \frac{1}{T}\sum_{i=1}^{K_n}\frac{P_i}{\rho_p A_{(d,\gamma)\text{-}i}|\mathbf{u}|_i} \approx \frac{1}{n}\sum_{j=1}^{n}\left(\frac{1}{\Delta t_{meso}|\mathbf{u}_{gr}|_j A_{gr\text{-}j}}\sum_{i=K_{j-1}+1}^{K_j}\frac{P_i}{\rho_p}\right)_j = \frac{1}{n}\sum_{j=1}^{n} q_{p\text{-}gr\text{-}j} \tag{9}$$

in which the particle velocity vector and cross-sectional area are removed from the summation on a micro level, and the volume of Group j is estimated as $V_{gr\text{-}j} = \Delta t_{meso}|\mathbf{u}_{gr}|_j A_{gr\text{-}j}$. In Eq. (9), the summed property of k_j particles are divided by the volume of the particle group, yielding an extensive volume-average. This type of volume-average, applied on particle groups, is similar to averaging over a control volume in two-fluid (Eulerian/Eulerian formulation) models of two-phase flows. Eq. (9) performs debias on the particle-group level (Bergenblock and Leckner, 2004), and not on the micro level, (see Fig. 2), which is favourable in cases when the residence times of particles are not measured with sufficiently high accuracy, such as could be the case for noisy Doppler signals, or when a few absolute values of particle velocity vectors $|\mathbf{u}|_i$ are close to zero, invalidating the use of Eq. (4b). In order to estimate the instantaneous q_p, the length scale of a group, $V_{gr}^{1/3}$ should be at least an order of magnitude larger than the particle diameter. The absolute value of the velocity vector of

a particle group and the mean cross-sectional area $A_{\text{gr-}j}$ of the particle group in Eq. (9) are estimated as ensemble averages of the particle data, which for Group j gives

$$|\mathbf{u}_{\text{gr}}|_j = \left| \sum_{i=K_{j-1}+1}^{K_j} m_i \mathbf{u}_i \Big/ \sum_{i=K_{j-1}+1}^{K_j} m_i \right|; \quad A_{gr\text{-}j} = \frac{1}{k_j} \sum_{i=K_{j-1}+1}^{K_j} A_{(d,\gamma)\text{-}i} \tag{10}$$

The mean values of Eq. (10) should be larger than their corresponding RMS values for Eq. (9) to be valid. Eqs. (9) and (10) also require measurement of all velocity-components contributing to the mean velocity of the particle group.

The mass-weighted velocity on a meso-scale (where meso-scale is either meso or group) is estimated as

$$\begin{aligned} \overline{U^m_{\text{meso-scale}}} \approx \overline{U^{c_v}_{\text{meso-scale}}} &= \left(\overline{q_{\text{p-meso-scale}}}\right)_{q=c_v u} \Big/ \left(\overline{q_{\text{p-meso-scale}}}\right)_{q=c_v} \\ &= \frac{1}{n}\sum_{j=1}^{n} \overline{(c_v u)_{\text{meso-scale-}j}} \Big/ \frac{1}{n}\sum_{j=1}^{n} \overline{(c_v)_{\text{meso-scale-}j}} \end{aligned} \tag{11}$$

where the time-average velocity results in a meso-scale ensemble average. The long-time average standard deviation on a meso-scale is simply taken as the ensemble RMS value of the property, $q_{\text{p-meso}}$ or $q_{\text{p-gr}}$,

$$\overline{q_{\text{p-meso-scale}}}' = \left(\frac{1}{n}\sum_{j=1}^{n} \left(q_{\text{p-meso-scale-}j} - \overline{q_{\text{p-meso-scale}}}\right)^2 \right)^{1/2} \tag{12}$$

and the RMS velocity is estimated as

$$\overline{U^m_{\text{meso-scale}}}' \approx \overline{U^{c_v}_{\text{meso-scale}}}' \approx \frac{\left(\frac{1}{n}\sum_{j=1}^{n} \left((c_v u)_{\text{meso-scale-}j} - \overline{(c_v u)_{\text{meso-scale}}}\right)^2 \right)^{1/2}}{\left(\frac{1}{n}\sum_{j=1}^{n} \left((c_v)_{\text{meso-scale-}j} - \overline{(c_v)_{\text{meso-scale}}}\right)^2 \right)^{1/2}} \tag{13}$$

The high-frequency content of an intensive property, filtered out by the inverse of Δt_{meso}, can be estimated by the RMS values of the meso-averages here written in agreement with Eq. (8), with their long-time average,

$$\overline{q_{\text{p-meso}}}' = \frac{1}{n}\sum_{j=1}^{n} \left(\frac{1}{\Delta t_{\text{meso}}} \left(\sum_{i=K_{j-1}+1}^{K_j} \left(\frac{P_i}{\rho_p V_{(d,\gamma)\text{-}i}} - \overline{q_{\text{p-meso-}j}} \right)^2 \Delta t_i \right)^{1/2} \right)_j \tag{14}$$

Two types of field equations have been given, capable of estimating up to second order moments of particle properties and velocity: (i) on a meso-level, Eqs. (8), (11)–(14) (performing sampling debias using the particle's transit time and inverse of the validation volume), and (ii) on a particle-group level, Eqs. (9), (11)–(13) (the inverse of the estimated particle-group volume compensates for the particle sampling procedure). For flows, in which the correlation of particle size and velocity or PDA validation volume is strong, the former approach (debias on a micro level), Eq. (8), is expected to perform better than the latter approach. On the other hand, if the PDA data is obtained from noisy Doppler signals, the particle-group method may give better estimations than the meso-approach, since for the particle-group method the instantaneous particle residence time is only used to statistically estimate the cross-sectional area, $A_{(d,\gamma)\text{-}i}$.

2.3. Decorrelation scheme

The influence of a window shift, Δt_j, (see Fig. 3), needed to enhance frequency resolution of a time series of values of a field property of particle groups can be achieved using a decorrelation scheme presented by Bergenblock and Leckner (2004). As illustrated in Fig. 4, the scheme applies the arithmetic mean of values of the property of w particle subgroups within the local averaging time, Δt_{meso}. Hence, the values of the property of particles are weighted towards the centre of the local averaging time (Δt_{meso}) and thereby the correlation of the successive values of the property of nearby located particle groups, separated by Δt_j, is reduced. The jth decorrelated and mean value of an intensive property using Eq. (8) can be written

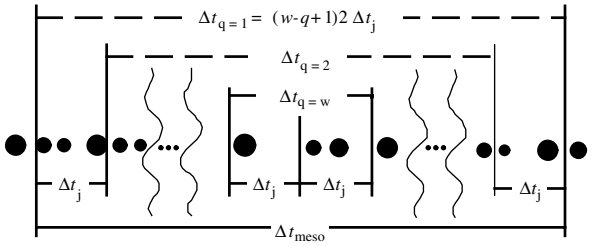

Fig. 4. Schematic drawing of the decorrelation scheme.

$$\langle \overline{q_{\text{p-meso-}j}} \rangle_j = \sum_{q=1}^{w} (\overline{q_{\text{p-meso-}j}})_q \Big/ w \tag{15}$$

where the number of sub-groups, w, within the jth particle group is

$$w = \Delta t_{\text{meso}}/(2\Delta t_j) \tag{16}$$

The local averaging time, Δt_q, for the estimation of the mean value of the property of each sub-group is

$$\Delta t_q = (w - q + 1)2\Delta t_j \tag{17}$$

where $q = 1, 2, \ldots, w$ and the mean of the intensive property of each sub-group becomes

$$(\overline{q_{\text{p-meso-}j}})_q = \frac{1}{\Delta t_q} \sum_{i=S_{j-1}+1}^{S_j} \frac{P_i \Delta t_i}{\rho_{\text{p}} V_{(d,\gamma)\text{-}i}} \tag{18}$$

where $S_j - S_{j-1}$ ($S_0 = 0$) is the number of particles within the sub-group and S_{j-1} is the total number of particles in the previous window shifts in the entire time series. Likewise, values of a property of particle-group averages calculated according to Eq. (9) can be decorrelated according to Eqs. (15)–(18).

3. Description of the simulation method

The PDA data post-processing algorithm proposed in Section 2, applicable to unsteady two-phase flow, will be validated by application on particle data produced by numerical simulation. Section 3.1 presents the essential features of a two-dimensional discrete particle code employed to simulate the fluid and particle dynamics of the two phases, and Section 3.2 describes the detection procedure of a particle in a simulated PDA probe volume. PDA validation criteria applied to detected particles are formulated in Section 3.3.

3.1. Discrete particle code

A numerical representation of a particle flow produces the test case to be evaluated by the PDA algorithm. The validation consists of a comparison between the particle flow, evaluated by the PDA algorithm, and the numerical representation of the same flow. In dilute gas/solids flows with an average solids volume fraction of the order of 10^{-3}, four-way coupled simulations are required to capture the features of the main flow (Elghobashi, 1994; Agrawal et al., 2001), since particles are likely to collide, and the disperse phase (e.g. streamers, clusters) modifies local flow fluctuations of the continuous phase. The 2D Eulerian/Lagrangian code used can handle such a flow situation. The code has been described previously (Helland et al., 2002; Soulas et al., 2004), and here it is only briefly presented. An Eulerian formulation for the gas phase solves the volume-averaged Navier–Stokes equation, and a Lagrangian formulation treats the disperse phase, based on the equations of motion. For the gas phase, the mass and momentum equations are

$$\frac{\partial(\varepsilon_{\text{G}}\rho_{\text{G}})}{\partial t} + \nabla \cdot (\varepsilon_{\text{G}}\rho_{\text{G}}\mathbf{u}_{\text{G}}) = 0 \tag{19}$$

$$\frac{\partial(\varepsilon_{\text{G}}\rho_{\text{G}}\mathbf{u}_{\text{G}})}{\partial t} + \nabla \cdot (\varepsilon_{\text{G}}\rho_{\text{G}}\mathbf{u}_{\text{G}}\mathbf{u}_{\text{G}}) = -\varepsilon_{\text{G}}\nabla \cdot (p_{\text{G}}\bar{\bar{I}}) + \nabla \cdot \varepsilon_{\text{G}}\overline{\overline{\tau_{\text{G}}}} + \varepsilon_{\text{G}}\rho_{\text{G}}\mathbf{g} - S_{\text{P}} \tag{20}$$

where $\mathbf{g}$ is the gravity acceleration, p_G the gas pressure, $\mathbf{u}_G$ the volume-averaged gas velocity, ε_G the void fraction, ρ_G the gas density, and $\overline{\overline{\tau_G}}$ the viscous stress. The coupling term between the gas and the particle phases, S_P, is the sum of the drag acting on each particle within the control volume in the fluid (Helland et al., 2002). Here, turbulence modelling is omitted, and the flow field is governed mainly by large scale fluctuations induced by the bluff body and the interaction between the phases.

The particles are modelled during their free-flight as

$$m_i \frac{\mathrm{d}\mathbf{u}_i}{\mathrm{d}t} = m_i \mathbf{g} + \mathbf{F}_{\mathrm{drag},i} - V_{\mathrm{solid},i} \nabla_P \tag{21}$$

where m_i, $\mathbf{u}_i$ and $V_{\mathrm{solid},i}$ are the mass, velocity, and volume of the ith particle. In Eq. (21), the terms on the right-hand side represent: gravity force, drag force between gas and particle, and gas pressure gradient force. Unsteady forces, Magnus lift and Saffman lift forces have all been neglected. The drag force is

$$\mathbf{F}_{\mathrm{drag},i} = \frac{C_{\mathrm{D},i}}{8} \pi d_i^2 \rho_G |\mathbf{u}_G - \mathbf{u}_i| (\mathbf{u}_G - \mathbf{u}_i) \varepsilon_G^{2-n} \tag{22}$$

where d_i is the particle diameter, n is taken as 4.7, and $C_{\mathrm{D},i}$ is the drag coefficient for a single sphere (i)

$$C_{\mathrm{D},i} = \begin{cases} \dfrac{24}{Re_p}\left(1 + 0.15 Re_p^{0.687}\right) & Re_p < 1000 \\ 0.44 & Re_p \geqslant 1000 \end{cases} \tag{23}$$

and Re_p is the particle Reynolds number

$$Re_p = \frac{\varepsilon_G |\mathbf{u}_G - \mathbf{u}_i| d_i}{\nu_G} \tag{24}$$

The void fraction, ε_G, of a computational cell in two dimensions is the ratio of the surface occupied by the gas and the surface of the cell. A pseudo three-dimensional method was used (Helland et al., 2002) to estimate the drag force of a sphere according to Eq. (22), with the void fraction,

$$\varepsilon_{G\text{-}3D} = 1 - \frac{2}{3}(1 - \varepsilon_{G\text{-}2D}) = 1 - \frac{2}{3}\left(\frac{1}{\Delta S}\sum_{i=1}^{N} S_i\right) \tag{25}$$

where S_i is the surface of particle i inside the fluid cell whose surface is ΔS. N particles are located in the fluid cell. The depth of the computational domain is one particle diameter. The influence on the void fraction of particles with centre positions located in adjacent cells may not be negligible if the volume of the fluid cell or the solids volume fraction is small. Thus, the pseudo-3D volume, $V_{\text{pseudo-3D-sphere-}i}$, representing the volume of the fraction of a sphere's volume inside a fluid cell in 3D, with corresponding area S_i in the fluid cell in 2D, is modified from the expression of Helland et al. (2002) (R is the radius of the sphere)

$$V_{\text{pseudo-3D-sphere-}i} = \frac{2}{3} S_i 2R \tag{26}$$

to the approximate formula,

$$V_{\text{pseudo-3D-sphere-}i} \approx \frac{2}{3} S_i 2\{R^2 - [\max(\min|x - x_0|, \min|y - y_0|)]^2\}^{1/2} \tag{27}$$

in which the centre (coordinates: x_0 and y_0) of the sphere may be located in an adjacent fluid cell, x and y are all coordinates of S_i. The square root term accounts for the decreased depth of $V_{\text{pseudo-3D-sphere-}i}$ if the particle's centre is outside the fluid cell. Thus, the 3D voidage of a fluid cell is estimated as

$$\varepsilon_{G\text{-}3D} \approx 1 - \frac{1}{\Delta V}\sum_{i=1}^{N} V_{\text{pseudo-3D-sphere-}i} \tag{28}$$

where $V_{\text{pseudo-3D-sphere-}i}$ is estimated from Eq. (27) and $\Delta V = \Delta S \cdot 2R$ is the volume of the fluid cell.

The dynamics of instantaneous non-frontal collisions are computed by means of a collision model (Wang and Mason, 1992) with friction based on three constants (Helland et al., 2002). The numerical solution technique of the Eulerian/Lagrangian code is based on the SIMPLE scheme and a non-staggered grid with pressure interpo-

lation. The integration of the conservation equations was performed by the Quick scheme in space and an implicit one in time. More details about the solution techniques can be found in Soulas et al. (2004).

3.2. Particle properties in the control and detection volumes

A control volume (CV) and a PDA detection volume (DV) (see Fig. 1a and b) are placed (at identical centre positions) in a flow. Averaging over the control volume is carried out for the particle phase as applied in two-fluid (Eulerian/Eulerian approach) models. Meso-scale time-averaging over DV, using the PDA data algorithm, and the Eulerian CV-averaging are compared. The size of the CV is small enough to capture the meso-scale structures in the flow, such as particle clusters and aggregates, while being much larger than the particle size. The time step for the CV-averaging ($\Delta t_{\mathrm{CV}} = 5 \times 10^{-3}$ s) was much smaller than the particle relaxation time.

Every time a part of a particle enters the simulated PDA detection volume, the particle and gas velocities (depending on the particle's centre position estimated by linear interpolation) are recorded together with the spatial position of the particle (which gives the solids volume concentration in the detection volume DV). The time step of the particle in the simulation is small ($\Delta t_{\mathrm{DV}} = 1 \times 10^{-5}$ s), which makes it possible to almost continuously follow the particle trajectories.

The computed time-mean and RMS solids volume concentrations of N samples during time T over the volume (Vol), where Vol is either CV or DV, are

$$\overline{c_{\text{v-Vol}}} = \frac{1}{T}\int_0^T \left(\sum_{i=1}^{N} c_{\text{v-Vol-}i}\right) \mathrm{d}t \approx \frac{\Delta t_{\mathrm{Vol}}}{T}\sum_{i=1}^{N} c_{\text{v-Vol-}i} = \langle c_{\text{v-Vol}} \rangle \tag{29}$$

$$\overline{c_{\text{v-Vol}}}' \approx \left[\frac{\Delta t_{\mathrm{Vol}}}{T}\sum_{i=1}^{N}\left(c_{\text{v-Vol-}i} - \overline{c_{\text{v-Vol}}}\right)^2\right]^{1/2} = c'_{\text{v-Vol}} \tag{30}$$

The time of each sample, Δt_{Vol}, is independent of the local instantaneous solids volume concentrations, $c_{\text{v-Vol-}i}$, yielding ensemble averages of the time-averages. The mass-weighted time-average velocities of particles (mean and RMS) are concentration-weighted, since Vol is constant,

$$\overline{u_{\mathrm{Vol}}^{\mathrm{m}}} = \overline{u_{\mathrm{Vol}}^{c_{\mathrm{v}}}} = \frac{\frac{1}{T}\int_0^T \left(\sum_{i=1}^{N} c_{\text{v-Vol-}i} u_{\text{Vol-}i}\right)\mathrm{d}t}{\frac{1}{T}\int_0^T \left(\sum_{i=1}^{N} c_{\text{v-Vol-}i}\right)\mathrm{d}t} \approx \frac{\frac{\Delta t_{\mathrm{Vol}}}{T}\sum_{i=1}^{N} c_{\text{v-Vol-}i} u_{\text{Vol-}i}}{\frac{\Delta t_{\mathrm{Vol}}}{T}\sum_{i=1}^{N} c_{\text{v-Vol-}i}} = \langle u_{\mathrm{Vol}} \rangle^{c_{\mathrm{v}}} \tag{31}$$

$$\overline{u_{\mathrm{Vol}}^{\mathrm{m}}}' = \overline{u_{\mathrm{Vol}}^{c_{\mathrm{v}}}}' \approx \frac{\left[\frac{\Delta t_{\mathrm{Vol}}}{T}\sum_{i=1}^{N}\left(c_{\text{v-Vol-}i} u_{\text{Vol-}i} - \overline{c_{\text{v-Vol}} u_{\mathrm{Vol}}}\right)^2\right]^{1/2}}{\left[\frac{\Delta t_{\mathrm{Vol}}}{T}\sum_{i=1}^{N}\left(c_{\text{v-Vol-}i} - \overline{c_{\text{v-Vol}}}\right)^2\right]^{1/2}} = u'^{c_{\mathrm{v}}}_{\mathrm{Vol}} \tag{32}$$

The particle size in the test case is uniform, and this avoids the difficulty of treating a cross-sectional area and length of the particle trajectory that depend on particle size. Instead, the governing Eqs. (2)–(14), are explored here as a function of the validation volume of the PDA, which depends on the trajectory angle (and not on particle size variation).

3.3. Validation criteria applied to detected particles

Four criteria are used to simulate fundamental validation requirements applied on a particle detected by a PDA system: (i) the particle's centre must be in DV, which is assumed to result in sufficient light scattering in a real PDA, (ii) the local swept length of a particle is required to be larger than, say, 10 μm to avoid multiple detection of the same particle along a DV-boundary, (iii) two succeeding particles must be separated by, say, at least 10 μs, and (iv) only one particle is allowed in DV during a particle trajectory. In accordance with the procedure of PDA signal processing, the instantaneous quantities (e.g. $u_{\text{DV-}i}$) of every valid particle passing DV are replaced with time-averages (u_i), saved at the arrival time of the particle's centre in DV. These values represent the entire particle trajectory, e.g. expressed for the particle velocity,

$$u_i = \frac{1}{\Delta t_i}\int_0^{\Delta t_i}\left(\sum_{i=1}^{p} u_{\mathrm{DV}\text{-}i}\right)\mathrm{d}t \approx \frac{\Delta t_{\mathrm{DV}}}{\Delta t_i}\sum_{i=1}^{p} u_{\mathrm{DV}\text{-}i} = \frac{1}{p}\sum_{i=1}^{p} u_{\mathrm{DV}\text{-}i} = \langle u_{\mathrm{DV}}\rangle \tag{33}$$

The time average velocity, u_i, once again, is calculated as an ensemble average, $\langle u_{\mathrm{DV}}\rangle$, of the p valid samples in DV for each detected and valid particle.

4. Test case

Fig. 1 shows the geometry of the test case (Fig. 1a) and close-ups of the simulated detection volume (Fig. 1b) as well as of a corresponding real PDA probe volume (Fig. 1d). Dimensions of the test case are given in Table 1 and operational parameters in Table 2. The domain is made pseudo 3D using the particle diameter as the third dimension. The average solids area concentration of 1.5×10^{-3} corresponds to a pseudo 3D solids volume concentration of about 1×10^{-3} according to Eq. (25). A bluff body, a flat plate in 3D, is positioned in the centre between the riser walls, perpendicular to the flow. The air inlet is modelled as a 1D uniform flow with a superficial velocity in the vertical direction of 1.2 m/s. The outlet at the top of the riser uses a continuity condition for the gas phase. The particles leaving at the top are simultaneously reintroduced at the bottom of the riser in random positions with zero velocities. The bluff body produces gas vortices in the wake with a vortex shedding frequency affecting the steadiness of the flow. If no particles were present, the frequency of the vortex shedding could be estimated to about 3 Hz from an assumed Strouhal number of 0.15 for the present configuration (flow passing around a flat plate with blockage caused by riser walls, with an approach gas velocity of 1.2 m/s and a blockage ratio of $w_t/w = 0.3$). The gas vortices create velocity fluctuations of the particle phase with similar characteristics as those of the gas phase, since the Stokes number based on large scale fluctuations of gas velocity is of the order of one. The particles tend to follow the fluctuations of the gas

Table 1
Geometry of the test case of Fig. 1

Riser	$w = 0.20$ m $h = 1.30$ m
Bluff body	$w_t = 0.06$ m Centre position: $x = 0.10$ m, $y = 0.20$ m
Control (CV) and detection (DV) volumes	$w_{CV} = 7.5$ mm $h_{CV} = 8.0$ mm $w_{DV} = 800$ μm $h_{DV} = 176$ μm $d = 120$ μm Centre position: $x = 0.06625$ m, $y = 0.31600$ m

Table 2
Operational parameters

Inlet vertical gas velocity, U_G (m/s)	1.2
Inlet vertical particle velocity, $u_{c\text{-}i}$ (m/s)	0
Temperature (K)	300
Gas viscosity, ν_G (m^2/s)	16.9×10^{-6}
Gas density, ρ_G (kg/m^3)	1.16
Solids diameter, d (m)	120×10^{-6}
Number of solids in the domain	35,000
Solids volume concentration	1×10^{-3}
Solids material density, ρ_p (kg/m^3)	2400
Solids terminal velocity (m/s)	0.66
Solids Reynolds number	5.0
Solids relaxation time, τ_p (s)	0.068
Total simulation time (s)	102.5

velocity, but because of particle inertia and gravity effects (such as present in this test case) there will be a slip velocity between the phases.

The control volume (CV) of the numerical simulation and its enclosed PDA detection volume DV (simulated by a rectangloid) are positioned downstream of the left-hand corner of the bluff body, where the flow is governed by vortex shedding. In the pseudo 3D configuration these volumes correspond to length scales $(CV)^{1/3}$ and $(DV)^{1/3}$ of about 16 and 3 particle diameters. The length of the $(CV)^{1/3}$, $16d$, is small but allows capturing particle clusters. The length of the $(DV)^{1/3}$, $3d$, is commonly used in optical set-ups of PDA systems in dense suspensions. The size of the detection volume is chosen as a trade off between the probability of having more than one particle occurrence at a time and getting a high particle sampling rate to enhance statistical estimates. The length-scale $3d$ is too short to estimate instantaneous values of intensive properties of particles, and thereby the length is also too short to calculate time-RMS values of such properties. Therefore, local time-averaging over Δt_{meso} is performed.

5. Results and discussion

Fig. 5 shows simulated instantaneous particle positions in the entire riser and in close-ups over the bluff body and the detection volume. As can be seen, particles located near each other tend to move in large groups/swarms with correlated velocities. The time series sampled in the control and detection volumes (see

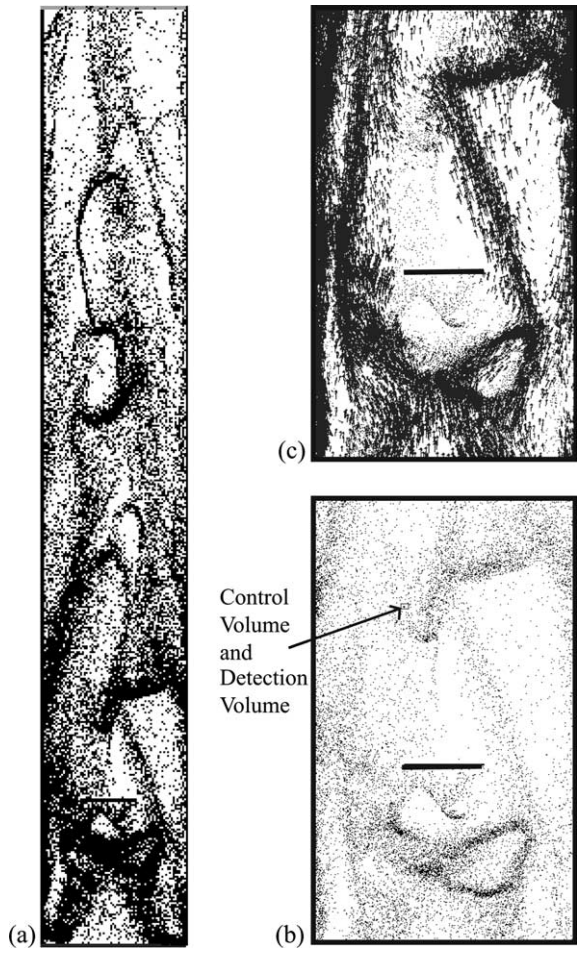

Fig. 5. Instantaneous particle positions in the riser; (a) entire riser, (b) close-up of the bluff body and the control and detection volumes, (c) particle velocity vectors with the same close-up as of (b). N.B. pixels, not particles, are shown.

Figs. 1a and b and 5b) are treated in Section 5.1 (gas velocities) and in Section 5.2 (particle properties). Section 5.3 presents the processed PDA type of time series on micro and meso-levels.

5.1. Gas velocities in the detection volume

Gas velocities from the numerical simulation were sampled in the detection volume, DV, in order to quantify the fluid dynamics in terms of velocity moments and Stokes number (based on an integral time scale of velocity fluctuations). Fig. 6 shows 2 s of gas and particle velocities, which strongly fluctuate with time. The two time series of vertical gas velocities seen in Fig. 6 were obtained: (i) at equidistant time intervals ($\Delta t_{CV} = 0.005$ s) at the CV/DV centre position, independent of whether particles were present or not, and (ii) at the location of the particle only at the time intervals ($\Delta t_{DV} = 1 \times 10^{-5}$ s) when particles were present in DV. The time-average gas velocity of the entire time series (102.5 s) depends on the information included in the averaging. It is lower in the second case (1.57 m/s), which represents the average gas phase velocity experienced by the particles, than in the first case (1.87 m/s), which is the average gas phase velocity. Obviously, if one wants to determine slip velocities with high accuracy, the gas velocities should be measured simultaneously with particle properties in the sampling volume, but this is not possible with the PDA technique. However, there are methods to deal with this problem: Prevost et al. (1996) estimated simultaneous fluid and particle velocities in the measuring volume using PDA and employed an interpolation technique to access the fluid velocity at the particle location. The RMS values of the two time series of vertical gas velocities are similar, 0.61 m/s ($\Delta t_{cv} = 0.005$ s) and 0.58 m/s ($\Delta t_{DV} = 1 \times 10^{-5}$ s). The integral time scale of the velocity fluctuation is estimated to $T_{i\text{-ugas}} = 0.1$ s by integrating an autocorrelation function based on equi-spaced ($\Delta t_{CV} = 0.005$ s) gas velocity fluctuations. Stokes number (St) can be estimated as particle relaxation time (τ_p) over integral time scale of the gas velocity fluctuations ($T_{i\text{-ugas}} = 0.1$ s). With $\tau_p = 0.068$ s for 120 μm glass spheres under the operating conditions of Table 2, this gives $St = 0.68$. For such an intermediate Stokes number (in the order of unity), obtained in a shear-dominated flow with coherent fluid structures, the large scale velocity fluctuations of the particle phase can be expected to somewhat exceed corresponding fluctuations of the gas phase (Hishida et al., 1992; Yang et al., 2000).

5.2. Particle properties in the control and detection volumes

Disperse phase is observed within the detection volume in the numerically simulated ($\Delta t_{DV} = 1 \times 10^{-5}$ s) time series (hereafter denominated NUM_SIM) during about 3.7% of the total simulation time (102.5 s). The instantaneous volume fractions of particles ($c_{v\text{-}DV\text{-}i}$) are shown in Fig. 7 for a few milliseconds, together with simultaneous vertical velocities of the particles ($u_{DV\text{-}i}$). The Path of particle (1) in Fig. 7a can be followed

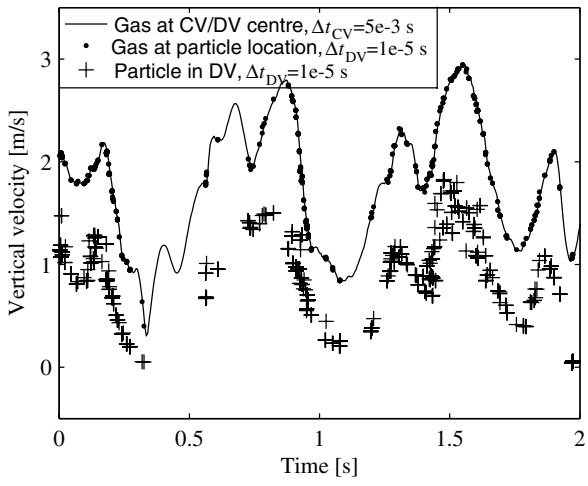

Fig. 6. Time series of simulated vertical gas and particle velocities in the detection volume.

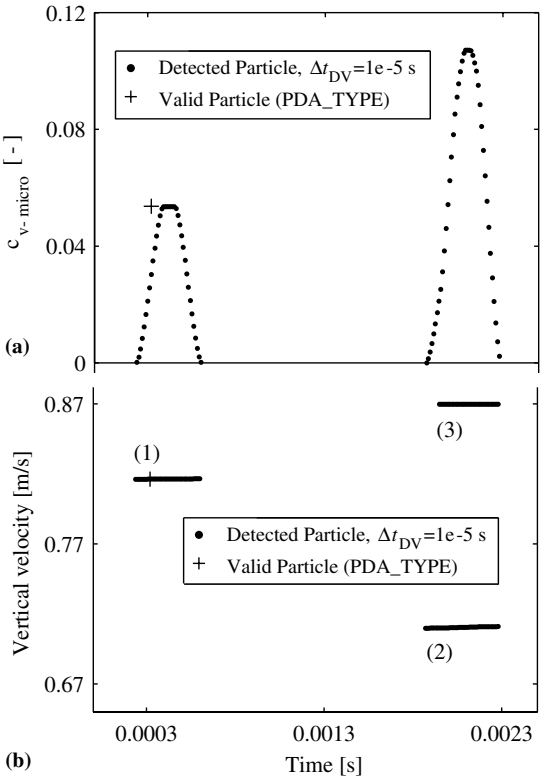

Fig. 7. NUM_SIM detected (●) and PDA_TYPE valid particles (+) in the detection volume. (a) Instantaneous solids volume concentrations in the detection and validation volumes, (b) vertical particle velocities in the detection volume. Only particle (1) is valid. The other particles (2 and 3) overlap in time.

in the $c_{\text{v-DV-}i}$ values; when a particle gradually enters the detection volume, $c_{\text{v-DV-}i}$ increases from zero to its plateau value 0.0535 when the entire particle is within DV. Thereafter $c_{\text{v-DV-}i}$ decreases to zero when the particle leaves the volume. This instantaneous solids volume concentration is not a good measure of the dynamics of the disperse phase, since it only varies from zero to its plateau value (0.0535). The solid volume concentration associated with a valid particle in Fig. 7a was estimated according to Eq. (33), which does not account for the particle trajectory-dependent validation volume. If the concentration is higher than 0.0535, more than one particle is present in DV, and these particles (labelled 2 and 3 in Fig. 7) are not valid. Fig. 7b shows that the velocities are close to constant during a passage through DV, as required by LDA. This is expected, because the residence times of particles in DV are much smaller than the relaxation time of a particle ($\tau_p = 0.068$ s).

In Table 3, all averages of the concentration in the detection volume c_v are shown. Calculated time-averages $c_{\text{v-DV}}$ of NUM_SIM for the entire detected time series according to Eqs. (29) and (30) (with $\Delta t_{\text{DV}} = 1 \times 10^{-5}$ s), yield mean and RMS values of 0.0011 and 0.0067, i.e. the time-average in the detection volume

Table 3
Time-averages of c_v over the detection/validation volume

Method	Equations	Variable	Mean (−)	RMS (−)	T_i (s)
NUM_SIM	(29) and (30)	$c_{\text{v-DV}}$	0.0011	0.0067	–
NUM_SIM	(29) and (30)	$c_{\text{v-CV}}$	0.0011	0.0013	0.045
PDA_TYPE	(4a) and (6)	$c_{\text{v-micro}}$	0.0010	0.0077	–
PDA_TYPE	(8), (12) and (15)	$c_{\text{v-meso}}$	0.0010	0.0013	0.047
PDA_TYPE	(9), (12) and (15)	$c_{\text{v-gr}}$	0.0010	0.0012	0.046
PDA_TYPE	(14) and (15)	$c'_{\text{v-meso}}$	0.0056	0.0048	0.054

Table 4
Averages of vertical velocities of particles (and gas) in the control and detection/validation volumes

Method	Equations	Variable	Mean (m/s)	RMS (m/s)	T_i (s)
NUM_SIM	(31) and (32)	$u^{\mathrm{m}}_{\mathrm{DV}}$	0.71	0.83	–
NUM_SIM	Ensemble	u_{CV}	0.77	0.50	0.074
NUM_SIM	(31) and (32)	$u^{\mathrm{m}}_{\mathrm{CV}}$	0.71	0.71	0.052
PDA_TYPE	(5) and (7)	$U^{\mathrm{m}}_{\mathrm{micro}}$	0.72	0.83	–
PDA_TYPE	(8), (11), (13) and (15)	$U^{\mathrm{m}}_{\mathrm{meso}}$	0.72	0.65	0.059
PDA_TYPE	(9), (11), (13) and (15)	$U^{\mathrm{m}}_{\mathrm{gr}}$	0.72	0.71	0.056
PDA_TYPE	Ensemble $\langle u\rangle^{\mathrm{m}}$, (1)	u	0.96	0.40	–
NUM_SIM	Ensemble	$u_{\mathrm{CV-Gas}}$	1.87	0.61	0.101

$c_{\text{v-DV}}$ is slightly larger than the time-average concentration of the entire riser (0.0010), and $c_{\text{v-DV}}$ agrees exactly with the NUM_SIM mean $c_{\text{v-CV}}$. The RMS value is about six times larger than the mean value: the estimation of c_{v} is made on too small a volume to correctly describe fluctuations in c_{v}, as confirmed by the corresponding NUM_SIM RMS value of 0.0013 obtained over CV.

Table 4 gives the average vertical velocities in the control and detection volumes. The NUM_SIM time-mean and RMS particle velocity $u^{\mathrm{m}}_{\mathrm{DV}}$ are 0.71 and 0.83 m/s according to Eqs. (31) and (32). The corresponding CV values $U^{\mathrm{m}}_{\mathrm{CV}}$ are 0.71 and 0.71 m/s. The over-prediction (0.12 m/s) in RMS value on the micro scale is due to its too short length ($3d$). The average difference in vertical velocity between the phases, i.e. the slip velocity, can be estimated from the vertical mean velocity of the gas experienced by the particles (1.57 m/s) and the mean particle velocity (0.71 m/s) to 0.86 m/s, which is larger than the terminal velocity of a particle (0.66 m/s). This is typical for flows of intermediate Stokes numbers: due to the gravity force, particles are preferentially swept to the lower side of eddies, and such particles obtain a high slip velocity (Wang and Maxey, 1993). Also in other works the slip velocity has been found to depend on local concentration of particles (Wang and Maxey, 1993; Aliseda et al., 2002).

5.3. Particle properties in the PDA validation volume

5.3.1. Micro scale

During 0.16% of the simulation time there were multiple particles in the detection volume. These particles are not valid. This percentage corresponds to 4.4% of the total time of particle occurrence (3.7 s) in the detection volume. Such a high value of rejected particles partly depends on the pseudo-3D assumption; if the width of the detection volume were equally large in the horizontal and in the third dimension (for the same size of detection volume as used in this pseudo-3D configuration), less frequent occurrence of multiple particles could be expected. This value (4.4%) somewhat exceeds the limit ($\sim 10^{-2}$) given by Edwards and Marx (1992), and hence the high rejection rate may affect estimates of moments of particle concentration. This effect is small, but observed in the present data. The four validation criteria of Section 3.3, applied on the time series of the detected particle ($\Delta t_{\mathrm{DV}} = 1 \times 10^{-5}$ s), result in an occurrence of valid particles during 1.65% of the simulation time with a total number of valid particles of 8025.

The properties (especially Δt_i and d_i) of a valid particle are subject to noise in a real measurement situation, and statistics are used to estimate the size of the validation volume according to Eq. (2). Therefore, the validation volume, $V_{(d,\gamma)\text{-}i}$, is calculated by dividing the trajectory lengths of valid particles into a maximum of 40 trajectory angle classes, with at least $n_j = 10$ particles per class for large trajectory angles according to Eq. (3). The instantaneous volume, $V_{(d,\gamma)\text{-}i}$, of Eq. (2) is obtained by fitting a fifth degree polynomial of the binned trajectory lengths (see Fig. 8), and by multiplying the interpolated length, $l_{(d,\gamma)\text{-interp.}}$, with the projected cross-sectional area, $A_{(d,\gamma)\text{-}i}$, of the validation volume. The projected cross-sectional area is calculated as the depth (d) of the pseudo 3D domain times the maximum projected width, A'_x or A'_y (see Fig. 1c),

$$A_{(d,\gamma)\text{-}i} = \max[A'_x, A'_y] \approx d \cdot \max[h_{\mathrm{D}} \sin\gamma_i, w_{\mathrm{D}} \cos\gamma_i] \tag{34}$$

The NUM_SIM particle velocities in the detection volume are replaced with valid velocities as if measured by PDA (hereafter denoted PDA_TYPE) according to the four criteria of Section 3.3 and Eq. (33). The

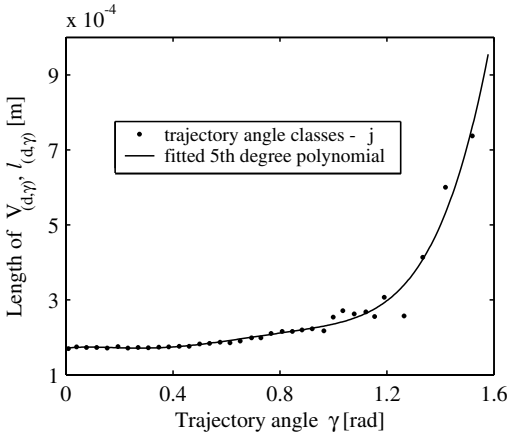

Fig. 8. Estimation of instantaneous length $l_{(d,\gamma)}$ of the validation volume $V_{(d,\gamma)}$ by curve-fitting a polynomial to the trajectory angle classes.

NUM_SIM velocities of a valid particle are saved as a single realization at the time of arrival of the particle's centre in the PDA detection volume to represent the entire passage through the validation volume (Fig. 7).

As summarized in Table 3, PDA_TYPE gives time-mean and RMS values of $c_{\text{v-micro}}$ of 0.0010 and 0.0077 (Eqs. (4a) and (6)). The mean value is slightly smaller than the NUM_SIM $\overline{c_{\text{v-DV}}}$ because of the validation criteria of the PDA processing, whereas the RMS value somewhat exceeds the NUM_SIM value. The corresponding PDA_TYPE vertical particle velocity, $\overline{U^{\text{m}}_{\text{micro}}}$ and its RMS, according to Eqs. (5) and (7), are 0.72 and 0.83 m/s, which agrees almost exactly with the NUM_SIM time-average values of U^{m}_{DV} 0.71 and 0.83 m/s (Eqs. (31) and (32)), Table 4. The agreement between the PDA_TYPE and NUM_SIM micro-scale time-moments proves the success of the PDA post-processing algorithm to estimate intensive particle properties in statistically steady state flows.

The ensemble mean of vertical velocities of particles are 0.96 m/s according to Eq. (1). Obviously, the ensemble average strongly over-predicts the vertical mean velocity, and it introduces a substantial high-velocity bias. This is so, since the ensemble average does not account for the particle sampling procedure of the LDA technique and fluctuations in particle concentration.

The RMS values of the processed particle velocities of PDA_TYPE (0.83 m/s) and of NUM_SIM (DV) (also 0.83 m/s) are greater than the fluctuations of the gas velocities (0.61 m/s) in the control volume. It is surprising that the difference is so large (0.22 m/s), although some discrepancy could be expected at such an intermediate Stokes number (0.68) in shear flows, containing coherent fluid structures (Hishida et al., 1992). The explanation is that the concentration-weighted velocities of particle flow are detected and processed over a volume that is not large enough to capture instantaneous particle concentration. Instead, the RMS values should be determined on a meso-scale.

5.3.2. Meso-scale

The local averaging time Δt_{meso} is taken equal to the integral time scale of fluctuations in solids volume concentration, 0.05 s, obtained from an integrated autocorrelation function (long-time mean value is removed) of NUM_SIM $c_{\text{v-CV}}$, illustrated in Fig. 9. This meso-scale averaging time (0.05 s) corresponds to a length scale of 14 particle diameters according to the third root of the meso-scale average $V_{\text{gr}} = \Delta t_{\text{meso}}|\mathbf{u}_{\text{gr}}|A_{\text{gr}}$, see Eq. (9). The length ($14d$) is very close to the length-scale of the CV ($16d$). The averaging time is a good choice as confirmed by the evaluation presented in Fig. 10, in which time-RMS values and integral time scales (T_i) are estimated on a meso-scale for solids volume fraction and velocity as a function of the local averaging time, Δt_{meso}. The PDA_TYPE RMS values of solids concentration, scaled with the NUM_SIM (CV) value, vary more with Δt_{meso} than the corresponding particle velocities. This is why Δt_{meso} is taken equal to the integral time scale of fluctuations in c_{v} (and not in velocity). The integral time scales increase strongly with longer Δt_{meso}, which introduces correlation into the meso-scale estimates of fluctuations of solids concentration and velocity.

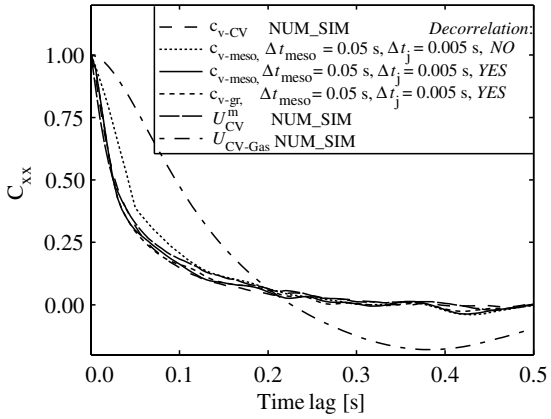

Fig. 9. Normalized autocorrelation functions C_{xx} of NUM_SIM (CV) and PDA_TYPE fluctuating solids volume concentration and of NUM_SIM (CV) fluctuating vertical velocities, with and without the decorrelation scheme.

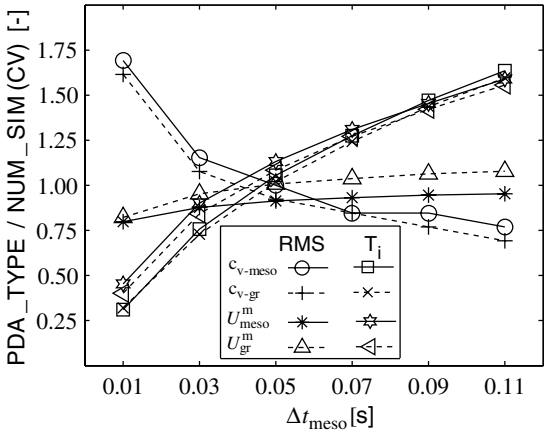

Fig. 10. Root mean square (RMS) values and integral time scales (T_i), related to NUM_SIM values over CV, of fluctuating solids volume concentration and of varying vertical particle phase velocity as a function of the local averaging time, Δt_{meso}. A window shift of $\Delta t_j = \Delta t_{meso}/10$ and the decorrelation scheme was used.

The estimated (scaled) meso-values of c_v and T_i as a function of Δt_{meso} intersect at about $\Delta t_{meso} = 0.05$ s (see Fig. 10), where the PDA_TYPE estimates agree well with the NUM_SIM (CV) values.

On a meso-scale, a window shift $\Delta t_j = 0.005$ s (chosen smaller than the average inter-particle time $\Delta t_{ip} = 0.013$ s) and the decorrelation scheme (with $w = 5$ particle sub-groups) according to Eq. (15) are introduced (see Figs. 3 and 4) to increase frequency resolution in the following estimates of particle properties. The influence of the window shift and the decorrelation scheme is negligible when estimating moments of intensive particle properties, but the influence on the spectral behaviour needs to be further investigated in detail. A validation of the decorrelation scheme is performed in Fig. 11, which shows power spectra of fluctuating solids volume concentration (long-time mean is removed) by comparing NUM_SIM (CV) and PDA_TYPE on a meso-scale. The power spectra were determined by the Welch method, in which the spectra are averaged from 32 sub-spectra (scaled by the sampling frequency). The sub-spectra were estimated with a Hanning window without overlap between the data segments. As can be seen in the figure, up to a frequency of about 10 Hz, all estimates coincide. For PDA_TYPE $c_{v\text{-meso}}$ and $c_{v\text{-gr}}$ with a window shift $\Delta t_j = 0.005$ s and the decorrelation scheme a frequency resolution is achieved of slightly less than 40 Hz (i.e. limited by the Nyquist critical frequency of the inverse mean inter-particle time $\Delta t_{ip} = 0.013$ s), whereas $c_{v\text{-meso}}$ without decorrelation

scheme only yields an acceptable spectral resolution to 10 Hz (i.e. limited by the Nyquist frequency applied on Δt_{meso}). Thus, the decorrelation scheme significantly decreases the correlation introduced by the over-sampling of the introduced window shift $\Delta t_j = \Delta t_{meso}/10$. A similar positive impact of the decorrelation scheme is confirmed by the autocorrelation functions of Fig. 9. The scheme preserves the decay in power spectral density of NUM_SIM (CV) of Fig. 11, without the spectral leakage that is present without adopting decorrelation.

Fig. 12 shows 0.2 s of instantaneous solids concentration: PDA_TYPE c_v on micro and meso-scales, with and without window shift and decorrelation, and c_v of NUM_SIM (CV). As expected, the instantaneous micro scale concentrations PDA_TYPE $c_{v\text{-meso}}$ (each value was obtained as particle volume divided by associated validation volume) are much higher than their corresponding meso-scale estimates $c_{v\text{-meso}}$ and $c_{v\text{-gr}}$ with and without window shift and decorrelation. The meso-scale time-mean and RMS concentrations according to Eqs. (8) and (12) of the entire time series (102.5 s) are $c_{v\text{-meso}}$ of 0.0010 and 0.0013. Thus, the mean values are identical on micro and meso-scales for PDA_TYPE of time series (Table 3). The RMS value on the micro scale, on the other hand, is much larger than its meso correspondence because the micro scale was too short to estimate fluctuations in c_v. The corresponding mean and RMS values of $c_{v\text{-gr}}$ according to Eqs. (9) and (12) are 0.0010 and 0.0012, which are in excellent agreement with the $c_{v\text{-meso}}$ values. The particle transit times, Δt_i, were not used explicitly in $c_{v\text{-gr}}$ (Eq. (9)), but the method nevertheless estimates c_v-moments just as well as the value

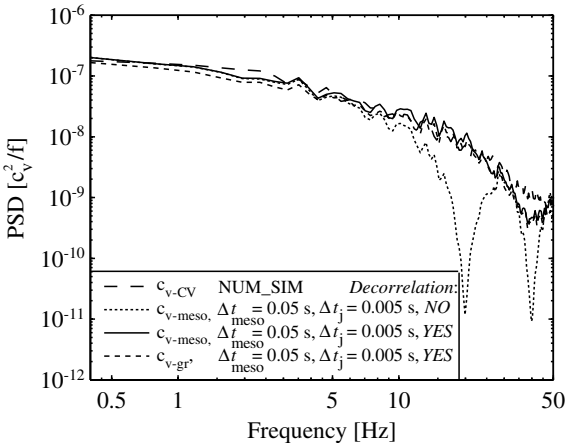

Fig. 11. Power spectra of NUM_SIM (CV) and PDA_TYPE fluctuating solids volume concentration, with and without the decorrelation scheme.

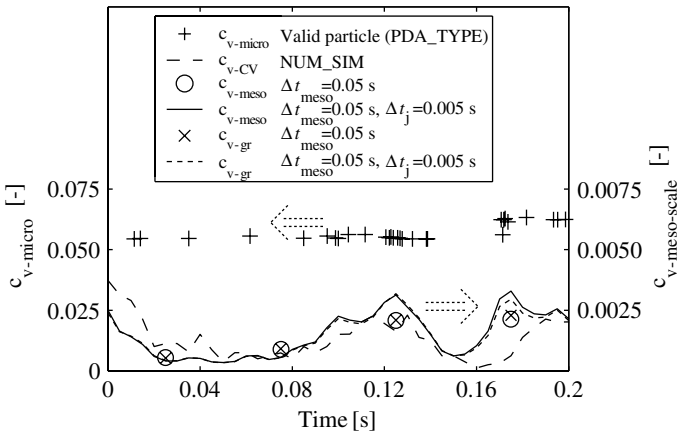

Fig. 12. Processed instantaneous NUM_SIM (CV) and PDA_TYPE solids volume concentrations during 0.2 s on micro and meso scales (Δt_{meso}), with and without the window shift (Δt_j) and decorrelation scheme.

of $c_{\text{v-meso}}$ (Eq. (8)). The local deviation from the meso Eq. (8) is estimated according to $c'_{\text{v-meso}}$ of Eq. (14), yielding time-mean and RMS values of 0.0056 and 0.0048. Thus, the RMS value $c_{\text{v-meso}}$ added to the mean $c'_{\text{v-meso}}$ of Eq. (14) gives 0.0069, which is close to the micro PDA estimate of RMS $c_{\text{v-micro}}$ 0.0077, which proves that the Δt_{meso} acts as a filter, with a cut-off frequency of $1/\Delta t_{\text{meso}} = 20$ Hz.

The meso-scale velocity $U^{\text{m}}_{\text{meso}}$ is calculated according to Eqs. (8), (11) and (15) as a meso-time-average with micro correction for velocity-dependent sampling volume and fluctuating particle concentration and results in time-mean and RMS values of 0.72 and 0.65 m/s. The mean value agrees exactly with the micro scale value $U^{\text{m}}_{\text{micro}}$ (Table 4), whereas the RMS value is, once again, smaller due to the filtering of the meso-averaging time, but it agrees well with the RMS fluctuation of NUM_SIM u^{m}_{CV} (0.71 m/s). If instead the velocity-dependent sampling rate and fluctuating particle concentration on a particle group scale are corrected according to Eqs. (9), (11) and (15), mean and RMS values of U^{m}_{gr} 0.72 and 0.71 m/s are obtained. These values coincide almost exactly with the NUM_SIM (CV) values. In fact they are closer to the CV values than the estimates of the micro correction approach ($U^{\text{m}}_{\text{meso}}$), since both the particle-group approach and the NUM_SIM (CV) employ volume-averaging on a scale much larger than the particle diameter.

To verify that there is a relation between local meso-scale velocity $U^{\text{m}}_{\text{meso}}$ and particle concentration $c_{\text{v-meso}}$, all dense particle groups (4.4% of all groups) were processed. The dense groups were sorted out from all groups by a rather arbitrary choice in cut off value of c_{v}: the distinguished groups should have c_{v}-values greater than two standard deviations (Sharma et al., 2000) of all samples of $c_{\text{v-meso}}$ above the mean value. The vertical mean velocity of the selected dense groups was calculated according to time-mean of $U^{\text{m}}_{\text{meso}}$ (Eqs. (8), (11) and (15)), which resulted in 0.37 m/s, i.e. about half of $\overline{U^{\text{m}}_{\text{meso}}}$. The corresponding RMS velocity of the dense groups was 0.82 m/s (slightly higher than the value of the entire phase ($\overline{U^{\text{m}}_{\text{meso}}} = 0.65$ m/s)). Hence, the vertical velocity of the denser particle groups is lower than the average particle velocity.

The facts that mono-disperse particles were used (the PDA validation volume does not depend on the particle diameter) and that dense particle groups have a much lower average vertical velocity than dilute groups (i.e. there is a strong correlation between velocity and concentration of particle groups) explain why the particle-group approach of Eq. (9), which uses volume averaging on a meso-scale, performs closer to the NUM_SIM (CV) results than the meso-approach (Eq. (8)) with a volume-average on a micro scale, see Eq. (4). Instead, if the flow investigated was governed mainly by local correlation between particle size and velocity, but still contains meso-scale flow structures, the meso-approach Eq. (8) is likely to be superior to the particle-group approach of Eq. (9) provided that the particle residence times are accurate.

6. Conclusions

A novel post-processing algorithm (a statistical estimator) of PDA data obtained in two-phase flow has been developed. A numerically computed test case with well-defined control (CV) and PDA detection (DV) volumes (without experimental noise) was examined to verify time-averaging with mass weighting and correction for the sampling procedure, performed by the statistical estimator and applicable to data (locally correlated) of low-speed, variable flow, but statistically steady. The PDA detection volume was positioned at the centre of the much larger control volume. Time-moments on micro and meso-scales of velocity and concentration of particles were determined by the estimator on a PDA time series (called PDA_TYPE) and compared with corresponding moments obtained by the numerical simulation (called NUM_SIM). In a wide range of applications, organized structures of particles (e.g. clusters) are known to form on a meso-scale and to move with a mean velocity that differs from the rest of the disperse phase. The estimator was able to process such correlated PDA data.

Fundamental validation requirements of a PDA system were applied on the NUM_SIM (DV) time series yielding the PDA_TYPE of time series. These different kinds of time series agree well. The PDA_TYPE averages of concentration ($\overline{c_{\text{v-micro}}}, \overline{c_{\text{v-meso}}}, \overline{c_{\text{v-gr}}}$) were identical but somewhat smaller than the NUM_SIM concentration $\overline{c_{\text{v-DV}}} = \overline{c_{\text{v-CV}}}$, the difference mainly depending on the occurrence of multiple particles in the detection volume which were discarded in the PDA_TYPE evaluation.

The ensemble average of PDA_TYPE particle velocities $\langle u \rangle^{\text{m}}$ was strongly high-velocity biased, and it should not be used for data of low-speed fluctuating flow. The statistical estimator applied on PDA_TYPE gives averages ($\overline{U^{\text{m}}_{\text{micro}}}, \overline{U^{\text{m}}_{\text{meso}}}, \overline{U^{\text{m}}_{\text{gr}}}$), which are not biased and very similar to the NUM_SIM $\overline{u^{\text{m}}_{\text{CV}}}$. The validation

volume of the PDA can be used to obtain average data, but it is too small (a characteristic length of about 3 particle diameters) to estimate instantaneous and then also time-RMS volume concentration of particles. To make up for the small volume, the PDA_TYPE was processed with a constant local averaging time on a meso-scale, Δt_{meso} (corresponding to an average length of 14 particle diameters (d), which is close to the length of the CV ($16d$)), and instantaneous particle volume fractions were successfully estimated. The value Δt_{meso} was chosen from the integral time scale of fluctuations in solids volume concentration, evaluating an integrated auto-correlation function of NUM_SIM (CV). In a real measurement situation, it can be difficult to accurately determine Δt_{meso}, since it may be hard to find out the correlation time of fluctuations in the intensive property with the shortest auto correlation time.

The PDA_TYPE RMS velocity of particles on a meso-scale ($\overline{U^{m}_{meso}}'$), with correction for the method of particle sampling of the PDA and the fluctuations in particle concentration on a micro scale, coincided well with the RMS of the velocity fluctuations in the particle phase ($\overline{U^{m}_{CV}}'$). In the case of particle transit times determined with insufficient accuracy (as by noisy Doppler signals), correction for the procedure of particle sampling and the variations in particle concentration should be performed on a particle group scale. The PDA_TYPE RMS velocity of particles ($\overline{U^{m}_{gr}}'$), with such a particle-group correction, agreed exactly with $\overline{U^{m}_{CV}}'$. Dense particle groups were found to have a much lower mean vertical velocity than dilute ones, which explains why the results of NUM_SIM (CV) and the PDA particle-group approach are in excellent agreement, since the spatial averaging of these methods correct for correlation of particle-group velocity and density on a meso-scale.

Power spectra and autocorrelation functions of PDA_TYPE solids concentration and velocity, processed on a meso-scale with a window shift and a decorrelation scheme, agree very well with corresponding NUM_SIM (CV) estimates.

The results prove that PDA data of the disperse phase, obtained in flow with fluctuating velocity and with locally correlated properties of particles, should be treated with a local averaging time (Δt_{meso}), to compensate for the small measuring volume of the PDA, for the estimation of fluctuations in intensive properties of particles. Thus, the estimator of PDA data has been numerically validated and the post-processing algorithm is recommended to be applied to data of real PDA measurements in unsteady two-phase flow.

References

Agrawal, K., Loezos, P.N., Syamlal, M., Sundaresan, S., 2001. The role of meso scale structures in rapid gas–solid flows. J. Fluid Mech. 445, 151–185.

Aliseda, A., Cartellier, A., Hainaux, F., Lasheras, J.C., 2002. Effect of preferential concentration on the settling velocity of heavy particles in homogeneous isotropic turbulence. J. Fluid Mech. 468, 77–105.

Bao, J., Soo, S.L., 1996. Measurement of particle flow properties in a suspension by a laser system. Int. J. Multiphase Flow 22, 143.

Bergenblock, T., Leckner, B., 2004. Velocity bias and concentration fluctuations in two-phase flow applications of phase Doppler particle analysis: a post-processing algorithm. In: Celata (Ed.), Proc. of 3rd International Symposium on Two-Phase Flow Modelling and Experimentation, Pisa, Italy. vol. II, pp. 843–850.

Bergenblock, T., Johnsson, F., Leckner, B., Onofri, F., Tadrist, L., 2004. Analysis of mesoscale structures in a circulating fluidized bed using a phase Doppler particle analyzer. In: Arena (Ed.), Proc. of 11th Conf. on Fluidization, Engineering Conf. Int., Paper HRD9.

Berkelmann, K.G., Renz, U., 1991. Gas and solid flow in the freeboard of a fluidized-bed combustor. Powder Technol. 68, 271–280.

Buchhave, P., 1975. Biasing errors in individual particle measurements with the LDA-counter signal processor. LDA-Symposium. Copenhagen, Denmark, pp. 258–278.

Buchhave, P., George, W.K., Lumley, J.L., 1979. The measurement of turbulence with the laser-Doppler anemometer. Ann. Rev. Fluid Mech. 11, 443–503.

Edwards, C.F., Marx, K.D., 1992. Analysis of the ideal phase-Doppler system: limitations imposed by the single-particle constraint. Atomization Spray 2, 319–366.

Elghobashi, S., 1994. On predicting particle-laden turbulent flows. Appl. Sci. Res. 52, 309–329.

Fuchs, W., Nobach, H., Tropea, C., 1994. Laser Doppler anemometry data simulation: application to investigate the accuracy of statistical estimators. AIAA J. 32, 1883–1889.

George, W.K., 1975. Limitations to measuring accuracy inherent in the laser Doppler signal. LDA-Symposium. Copenhagen, Denmark, pp. 20–63.

Hamdullahpur, F., Mackay, G.D.M., 1986. 2-Phase flow behavior in the freeboard of a gas-fluidized bed. AICHE J. 32, 2047–2055.

Hardalupas, Y., Horender, S., 2001. Phase Doppler anemometer for measurements of deterministic spray unsteadiness. Part. Part. Syst. Char. 18, 205–215.

Helland, E., Occelli, R., Tadrist, L., 2002. Computational study of fluctuating motions and cluster structures in gas-particle flows. Int. J. Multiphase Flow 28, 199–223.

Hishida, K., Ando, A., Maeda, M., 1992. Experiments on particle dispersion in a turbulent mixing layer. Int. J. Multiphase Flow 18, 181–194.

Ibsen, C.H., Solberg, T., Hjertager, B.H., 2001. Evaluation of a three-dimensional numerical model of a scaled circulating fluidized bed. Ind. Eng. Chem. Res. 40, 5081–5086.

Ibsen, C.H., Helland, E., Hjertager, B.H., Solberg, T., Tadrist, L., Occelli, R., 2004. Comparison of multifluid and discrete particle modelling in numerical predictions of gas particle flow in circulating fluidised beds. Powder Technol. 149, 29–41.

Levy, Y., Lockwood, F.C., 1983. Laser Doppler measurements of flow in freeboard of a fluidized-bed. AICHE J. 29, 889–895.

Mathiesen, V., Solberg, T., Hjertager, B.H., 2000. An experimental and computational study of multiphase flow behavior in a circulating fluidized bed. Int. J. Multiphase Flow 26, 387–419.

McLaughlin, D.K., Tiederman, W.G., 1973. Biasing correction for individual realization of laser anemometer measurements in turbulent flows. Phys. Fluids 16, 2082–2088.

Pope, S.B., 1985. PDF methods for turbulent reactive flows. Prog. Energ. Combust. Sci. 11, 119–192.

Prevost, F., Boree, J., Nuglisch, H.J., Charnay, G., 1996. Measurements of fluid/particle correlated motion in the far field of an axisymmetric jet. Int. J. Multiphase Flow 22, 685–701.

Roisman, I.V., Tropea, C., 2001. Flux measurements in sprays using phase Doppler techniques. Atomization Spray 11, 667–669.

Saffman, M., 1987. Automatic calibration of LDA measurement volume size. Appl. Optics 26, 2592–2597.

Samuelsberg, A., Hjertager, B.H., 1996. An experimental and numerical study of flow patterns in a circulating fluidized bed reactor. Int. J. Multiphase Flow 22, 575–591.

Sharma, A.K., Tuzla, K., Matsen, J., Chen, J.C., 2000. Parametric effects of particle size and gas velocity on cluster characteristics in fast fluidized beds. Powder Technol. 111, 114–122.

Sommerfeld, M., Qiu, H.-H., 1995. Particle concentration measurements by phase-Doppler anemometry in complex dispersed two-phase flows. Exp. Fluids 18, 187–198.

Soulas, J., Occelli, R., Simonin, O., Tadrist, L., Reiling, V., 2004. Comparison of dense gas–solid fluidized bed predictions from hard-sphere discrete particle and two-fluid continuum modeling approaches. In: Matsumoto, Y., Michaelides, E.E., Fabre, J. (Eds.), 5th International Conference on Multiphase Flow, ICMF'04. Yokahama, Japan, Paper No. 353.

Tropea, C., 1987. Turbulence-induced spectral bias in laser anemometry. AIAA J. 25, 306–309.

van de Wall, R.E., Soo, S.L., 1994. Measurement of particle cloud density and velocity using laser devices. Powder Technol. 81, 269–278.

van de Wall, R.E., Soo, S.L., 1997. Measurement of transport properties of a gas–solid suspension using phase Doppler anemometry. Powder Technol. 94, 141–151.

Van den Moortel, T., Santini, R., Tadrist, L., Pantaloni, J., 1997. Experimental study of the particle flow in a circulating fluidized bed using a phase Doppler particle analyser: a new post-processing data algorithm. Int. J. Multiphase Flow 23, 1189–1209.

Van den Moortel, T., Azario, E., Santini, R., Tadrist, L., 1998. Experimental analysis of the gas-particle flow in a circulating fluidized bed using a phase Doppler particle analyzer. Chem. Eng. Sci. 53, 1883–1899.

Wang, Y., Mason, M.T., 1992. Two-dimensional rigid body collisions with friction. J. Appl. Mech. 59, 635–642.

Wang, L.-P., Maxey, M., 1993. Settling velocity and concentration distribution of heavy particles in homogeneous isotropic turbulence. J. Fluid Mech. 256, 27–68.

Wang, T., Lin, Z.J., Zhu, C.M., Liu, D.C., Saxena, S.C., 1993. Particle-velocity measurements in a circulating fluidized-bed. AICHE J. 39, 1406–1410.

Werther, J., Hage, B., Rudnick, C., 1996. A comparison of laser Doppler and single-fibre reflection probes for the measurement of the velocity of solids in a gas–solid circulating fluidized bed. Chem. Eng. Process. 35, 381–391.

Yang, Y.L., Jin, Y., Yu, Z.Q., Wang, Z.W., 1992. Investigation on slip velocity distributions in the riser of dilute circulating fluidized-bed. Powder Technol. 73, 67–73.

Yang, X., Thomas, N.H., Guo, L.J., 2000. Particle dispersion in organized vortex structures within turbulent free shear flows. Chem. Eng. Sci. 55, 1305–1324.

Zhang, Y.F., Arastoopour, H., 1995. Dilute fluidized cracking catalyst particles—gas-flow behavior in the riser of a circulating fluidized-bed. Powder Technol. 84, 221–229.